Journal of Photochemistry and Photobiology A: Chemistry 202 (2009) 39–47

Contents lists available at ScienceDirect

Journal of Photochemistry and Photobiology A: Chemistry

journal homepage: www.elsevier.com/locate/jphotochem

Photocatalytic and photoelectrochemical studies on N-doped TiO_2 photocatalyst

Xintong Zhang[a,c], Keizo Udagawa[b], Zhaoyue Liu[a], Shunsuke Nishimoto[a], Changshan Xu[c], Yichun Liu[c], Hideki Sakai[b], Masahiko Abe[b], Taketoshi Murakami[a], Akira Fujishma[a,*]

[a] Kanagawa Academy of Science and Technology, West 614, KSP Buildings, 3-2-1 Sakado, Takatsu-ku, Kawasaki, Kanagawa 213-0012, Japan
[b] Faculty of Science and Technology, Tokyo University of Science, 2641 Yamazaki, Noda 278-8510, Japan
[c] Center for Advanced Optoelectronic Functional Materials Research, Northeast Normal University, Changchun 130024, People's Republic of China

ARTICLE INFO

Article history:
Received 22 May 2008
Received in revised form
30 September 2008
Accepted 13 November 2008
Available online 25 November 2008

Keywords:
TiO_2
Nitrogen doping
Photocatalysis
Photoelectrochemistry

ABSTRACT

One of the commercial N-doped TiO_2 powders (Sumitomo Chemicals, TPS 201) was studied as a model material by photocatalytic and photoelectrochemical methods in order to evaluate the photoactivity of N-doped TiO_2 materials and the possibility of their applications in solar photocatalysis. The N-doped TiO_2 powder (TPS) was able to degrade and mineralize phenol under solar or visible light (VL) irradiation, and the degradation rate was strongly dependent on the suspension concentration. Photoelectrochemical studies showed that the VL-irradiated TPS electrode was able to oxidize water, phenol, as well as maleic acid, an open-ring oxidized product of phenol, consistent with the results of photocatalytic studies. Calcining the TPS powder at/over 773 K was found to lower the absorption in the VL region and the photocatalytic activity under VL irradiation, but improve the photocatalytic activity under solar irradiation, suggesting that the mid-gap states introduced by nitrogen doping also worked as recombination centers. Deposition of Pt (0.2 wt%) on the TPS photocatalyst thus greatly increased the degradation rate of phenol under either solar or VL irradiation due to the suppression of charge recombination, and the degradation rate was found to be higher than a pristine TiO_2 photocatalyst (ST-01, anatase) either with or without loading of Pt. The potential application of the N-doped TiO_2 in solar photocatalysis was discussed on the basis of above-mentioned studies.

1. Introduction

Since the first report of photo-splitting water on a TiO_2 electrode by Fujishima and Honda [1], extensive research has been carried out on TiO_2 materials for the purpose of solar energy conversion [2–6] and environmental cleanup [7–13], owing to their photoactivity, high corrosion resistance and nonhazardous nature. The TiO_2 material has a wide band gap, 3.2 eV for anatase and 3.0 eV for rutile, which allows the material to absorb ultraviolet light (~6% of solar energy) but to be transparent for most of the solar irradiation. This obviously restricts the solar energy applications of the material, for example in remediation of aquatic environment.

Recently, it has been reported that the TiO_2 material, when doped with nonmetal elements such as N [14–22] C [23–26], S [27–29] B [30], and F [31,32], etc., exhibits red-shifted absorption edge. Among of them, N-doped TiO_2 is the most studied material. Asahi et al. reported that a nitrogen-doped TiO_2 film prepared by the sputtering method exhibited an absorption threshold at 500 nm, and could decolorate methylene blue solution and decompose gaseous acetaldehyde under visible irradiation [14]. Later studies showed that TiO_2 could be doped with nitrogen by various physical and chemical methods [15–22]. Both substituted and interstitial nitrogen dopants were responsible for the red-shifted absorption threshold, as proven by the X-ray photoelectron spectroscopy (XPS) [14–22], ultraviolet photoemission spectroscopy (UPS) [33,34], electron paramagnetic resonance (EPR) [35,36], as well as density functional theory (DFT) calculations [34–36].

However there are still issues concerning the photoactivity of the N-doped TiO_2. Asahi et al. claimed that nitrogen doping offered TiO_2 the photoactivity under visible light, without degradation of the photoactivity under UV light [14]. But some later studies suggested that nitrogen doping, though offered TiO_2 the photoactivity under visible light (VL) irradiation, yet it weakened the photoactivity of the TiO_2 material for decomposition of acetaldehyde and splitting of water under UV irradiation [16–18]. There have been several reports even claimed that nitrogen doping did not render TiO_2 be photoactive under VL irradiation [19,37]. Besides these, very little report has concerned the solar photocatalytic properties of the material contributed by UV- and VL-stimulated processes together, which is one of the most important issues related to environmental remedy applications. Therefore, it appears to be urgent for us to make clear how nitrogen dopant influences the photocatalytic properties TiO_2 materials under either VL or solar irradiation, and how we can do to improve the photoactivity of N-doped TiO_2. To

* Corresponding author. Tel.: +81 44 819 2020; fax: +81 44 819 2038.
E-mail address: fujishima@newkast.or.jp (A. Fujishma).

1010-6030/$ – see front matter © 2008 Elsevier B.V. All rights reserved.
doi:10.1016/j.jphotochem.2008.11.007

achieve the aims, commercially available N-doped TiO_2 materials are obviously preferred in study, since they can be obtained in a large amount with the same preparation history.

In the present study, we selected a commercial N-doped TiO_2 powder, TPS 201, made by Sumitomo Chemicals (TPS) as the model photocatalyst, and studied its photoactivity under VL and solar irradiation by photocatalytic and photoelectrochemical methods. We expect the combination of photocatalytic and photoelectrochemical methods could help us to understand factors that influence the photoactivity of the N-doped TiO_2 materials. All photocatalytic experiments were conducted using a solar simulator as the light source and phenol, a nonbiodegradable and light-stable pollutant, as the substrate, in order to evaluate the potential applications of N-doped TiO_2 materials in solar photocatalysis. Platinum was examined as a potential cocatalyst to improve the photoactivity of N-doped TiO_2 materials under VL and/or solar irradiation, as what was often done in UV-stimulated TiO_2 photocatalysis [38–40]. Moreover, we also studied the thermal stability of the N-doped material, an important parameter should be considered in immobilization of the material.

2. Experimental

2.1. Chemicals

N-doped TiO_2 powder (TPS 201) was obtained from Sumitomo Chemicals. Pristine TiO_2 powder (ST-01, anatase) was obtained from Ishihara Sangyo. Phenol, maleic acid, hydrogen hexachloroplatinate, and methanol were obtained from Wako. Acetylacetone and Triton-100 were obtained from Aldrich. These chemicals were used as received without purification. Deionized water was used in all the experiments.

2.2. Preparation of photocatalysts

Pt-deposited pristine or N-doped TiO_2 powders were prepared by the reported method with a little modification [41]. Typically, 7 g N-doped TiO_2 powder was ultrasonically dispersed in 350 mL deionized water. The suspension was purged with N_2 under magnetic stirring for 30 min. Then, calculated amount of H_2PtCl_6 solution was added to the suspension, together with 1 mL methanol. The suspension was irradiated with UV light (Hayashi UV-310, 20 mW cm^{-2}) under stirring for 2 h. After the reaction, the N-doped TiO_2 powder was collected by repeated centrifugation and washing with deionized water. The powder obtained after drying was grey or black color, in contrast to the yellow color before the photoreaction, which is an evidence of deposition of Pt on the powder.

Four kinds of calcined N-doped TiO_2 powders were prepared by heating the commercial sample in air at 400 °C, 500 °C, 600 °C, and 700 °C for 1 h, respectively. The calcined samples were named by the calcination temperature as TPS 400, TPS 500, TPS 600, and TPS 700, respectively. The non-calcined sample was named as TPS for comparison.

2.3. Preparation of film electrodes

4 g TPS powder was ground together with 12 mL water, 0.5 mL acetylacetone, and 20 μL Triton-100 in a mortar to prepare paste. The paste was coated on conductive glass plates (F-doped SnO_2, Nippon Sheet Glass, 10 Ω/□) with a glass rod by the doctor-blade method. After drying in air for 30 min, the films were pressed at a hydraulic pressure of 12 MPa to get desired mechanical strength, and were subsequently heated at 673 K for 30 min to remove organic residuals. Finally, the conductive glass plates were connected with copper wires with silver conductive paste and all the conductive area was sealed with epoxy resin. The films were about 5 μm-thick, as measured with a laser profile microscope (Keyence, VF7510).

2.4. Photocatalytic degradation of phenol

A solar simulator (Yamashita Denso, YSS-100A) was used in all photocatalytic experiments to provide AM 1.5 simulated solar irradiation (100 mW cm^{-2}). Cutoff filters (Fuji Films, A4 size), such as SC42 filter (λ > 400 nm), SC46 filter (λ > 450 nm), SC58 filter (λ > 565 nm), etc. were used in some experiments to select the wavelength range of simulated solar light.

Photocatalytic experiments were carried out in a water-jacketed Pyrex glass vessel covered with a quartz plate. The reactor vessel was irradiated with simulated solar light from top. Typically, 3 g (or 0.3 g) N-doped TiO_2 powder and 147 mL deionized water were fed in the reactor vessel, and were treated ultrasonically for 30 min. Then, 3 mL phenol stock solution (1 g L^{-1}) was added into the reactor vessel to reach a concentration of ~20 mg L^{-1}, and the pH of the mixture suspension was adjusted to 5 with 0.1 mol L^{-1} HCl solution. After storage in dark for 30 min, the reactor vessel was irradiated with simulated solar light. The temperature of the suspension was kept at room temperature with circulated water. The degradation of phenol as a function of irradiation time was followed with a HPLC chromatograph (Shimadzu LC-2010C_{HT}; Column: Synergi 4 μ Fusion-PR 80A, Phenomenedx) using a mobile phase of methanol/H_2O (1:1 by volume), and a total organic carbon analyzer (TOC, Shimadzu TOC-V_{CSH}). The samples were filtered with 0.2 μm filtering membrane (Millipore) before HPLC and TOC measurements.

2.5. Photoelectrochemical measurements

The N-doped TiO_2 film electrode was fixed in a 100 mL pyrex glass electrochemical cell that had a quartz window in sidewall. A platinum wire was used as counter electrode, and an Ag/AgCl electrode was used as reference. A N_2-saturated 0.1 mol L^{-1} sodium perchlorate solution (pH ~ 5) was used as supporting electrolyte. The electrodes were assembled with an Automatic Polarization System (Hokuto Denso, HZ-5000) to form an electrochemical circuit. The N-doped TiO_2 film electrode was irradiated from the backside of the conductive glass plate with a 350 W Xe lamp (Yamashita Denso, MLH-300; light intensity: 500 mW cm^{-2}), and the electrolyte solution was mechanically stirred and degassed by purged with N_2 before and during all the experiments.

Several kinds of cutoff filters (Fuji Films), including SC42 (λ > 400 nm), SC46 (λ > 450 nm), SC52 (λ > 500 nm), SC58 (λ > 565 nm) filters, were put in the light path in some cases to study the dependency of photocurrent on excitation wavelength. The influence of organic substances, such as phenol and maleic acid, on the observed photocurrent response was also studied by adding these substances to the electrolyte solution with a concentration of 100 mg L^{-1}.

2.6. Characterizations

Particle size of the N-doped TiO_2 powder was measured with a transmission electron microscope (TEM, Topcon EM-002B) at an accelerating voltage of 200 kV. The crystal morphology of the powder was measured with a X-ray diffractometer (Rigaku RINT1500) with graphite-monochromatized Cu Kα radiation, and a Raman spectrometer (JY HR800). Grain sizes of the TPS and calcined powders were estimated from the (1 0 1) diffraction peak by the Scherer equation, using sintered α-quartz powder (35 μm) as a reference. The BET surface area of the powder was measured with a BET surface area analyzer (Macsorb HM-1220). The diffuse reflection spectra were recorded with a UV–vis spectrophotometer (Shi-

madzu 2450) equipped with an integrated sphere. The composition of the powder was analyzed with X-ray photoelectron spectroscopy (XPS, S-Probe ESCA, Surface Science Instruments) using Al Kα radiation. Before XPS measurements, the powder was sputtered with Ar^+ for 10 min to remove surface contamination of N-contained species that may be introduced during chemical preparation, or by chemiadsorbed N_2 [42]. This procedure was considered to be important to accurately assign the XPS spectra obtained.

3. Results and discussion

3.1. Properties of the N-doped TiO_2 photocatalyst

The N-doped TiO_2 powder (TPS) used in this study is a commercial product of Sumitomo Chemicals, which was prepared by the wet-chemical method. According to the manufacturer's data, the average particle size of the TPS powder is 12 nm, which is consistent with our TEM observations (Fig. 1). The powder crystallized well in anatase structure, as proven by the XRD pattern (Fig. 2a), and had a BET surface area of 97.4 $m^2\,g^{-1}$. The Raman spectrum of the TPS film showed characteristic phonon peaks of anatase at 634, 515, 395, 197, and 144 cm^{-1} (Fig. 2b) [43,44]. The XPS spectrum of the TPS powder after Ar^+ sputtering showed a peak at 399.6 eV which could be assigned to N1 s band of interstitial doped nitrogen atoms (Fig. 2c) [35,36], and a weak feature around 396 eV which could be assigned to N1 s band of substituted nitrogen atoms [14,33,34]. The latter was much weaker than the former, and was almost buried by noise. The nitrogen atoms were estimated to replace 1% of lattice oxygen by the XPS data.

$$F(R) = \frac{(1-R)^2}{2R} \quad (1)$$

The yellow-colored TPS powder exhibited apparent red-shift threshold (~540 nm) in the diffuse reflection (DR) spectra (Fig. 3a) and tail at even longer wavelength, compared to pure anatase TiO_2 powder. Such a DR spectrum was similar as the reported data of N-doped TiO_2 powders. The DR spectrum was converted by the Kubelka-Munk function (Eq. (1)) to generate the absorption spectrum; the converted spectrum was also shown in Fig. 3a. The light absorption onset of TPS powder is ca. 540 nm as shown in the figure, but the absorption in the spectral region over 400 nm is one or two orders lower than that in the UV spectral region. This may influence the activity of the TPS powder under VL irradiation. The band gap of the TPS powder estimated from the steeply rising absorption was 3.12 eV (Fig. 3b), which was a bit red-shift from the 3.18 eV of anatase TiO_2 (ST-01, Ishihara Sangyo). This small red-shift of 0.06 eV is probably contributed by oxygen vacancies introduced by nitrogen doping, whose position is below the conduction band edge, as suggested by Lin et al. [45]

Table 1
Initial rate constants of phenol degradation in the TPS suspension (20 g L^{-1}) under various irradiation conditions.

	Solar light	λ > 400 nm	λ > 450 nm	λ > 565 nm
Rate constant/min^{-1}	6.8×10^{-3}	4.2×10^{-3}	2.9×10^{-3}	3.2×10^{-4}

3.2. Photocatalytic activity of TPS powder

The TPS powder was able to degrade phenol under solar irradiation, as shown in Fig. 4 and Table 1. The decrease of phenol concentration was accompanied by the appearance of intermediate products with shorter retention time. These intermediate products were assigned to hydroquinone, benzoquinone, and some opening oxidized products of phenol. The total organic carbon (TOC) was also decreased in the suspension as a function of irradiation time, though the decreasing trend was slower than that of phenol, indicating the TPS powder could completely mineralize phenol under solar irradiation.

The simulated AM1.5 solar irradiation spans a wide wavelength range from 310 nm to 2.5 μm, and contains UV light in a portion of ~6%. We selected the spectral range of solar irradiation with different cutoff filters, and found that the visible part of solar light could stimulate the photocatalytic degradation of phenol by the TPS powder (Fig. 4 and Table 1). The powder exhibited activity for phenol degradation under the irradiation of λ > 400 nm and λ > 450 nm; but only trivial decrease in phenol concentration was observed under the irradiation of λ > 565 nm, as shown in Fig. 4. The TOC results showed that the TPS powder was able to mineralize phenol under the VL irradiation (λ > 400 nm).

We also studied the influence of TPS concentration on the photocatalytic degradation of phenol, and did not observe the saturated degradation rate in a concentration range of 0.1–50 g L^{-1}. In contrast, pristine TiO_2 photocatalyst often showed saturated degradation rate over a concentration of 0.2 g L^{-1} [46]. We compared the degradation rates of phenol at two concentrations (2 g L^{-1} and 20 g L^{-1}) of the TPS powder under different irradiation conditions (Table 2), and found that the unsaturation phenomenon was mainly contributed by the VL-stimulated degradation. This is reasonable considering the relatively weak VL absorption of the TPS powder (Fig. 3a)

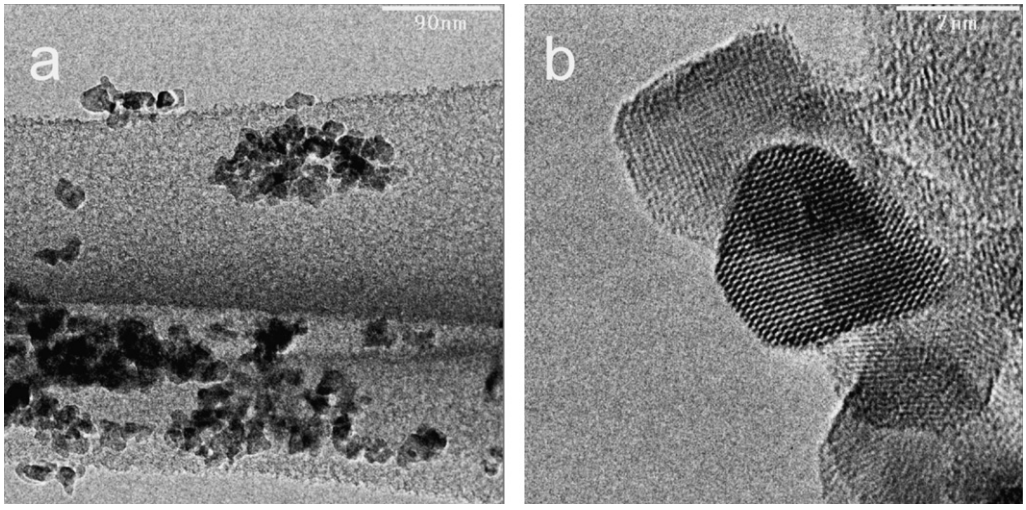

Fig. 1. TEM images of the TPS powder. The bars in a) and b) correspond to 90 nm and 7 nm, respectively.

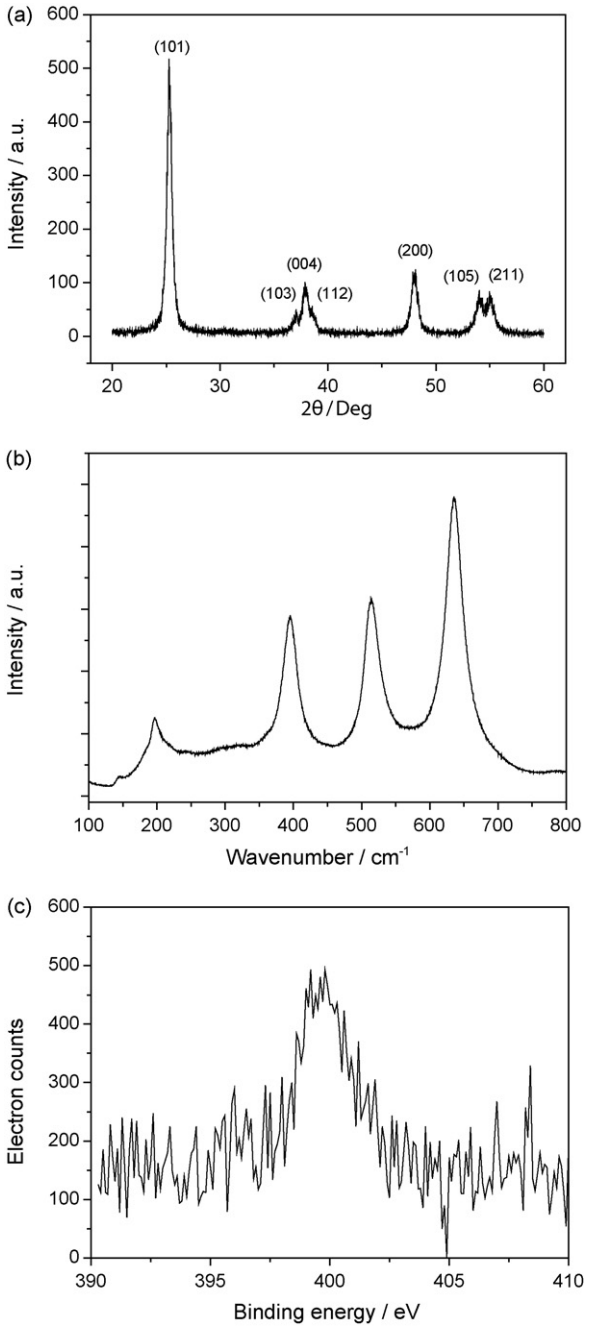

Fig. 2. a) XRD pattern, b) Raman spectrum, and c) N1 s XPS spectrum of the TPS powder.

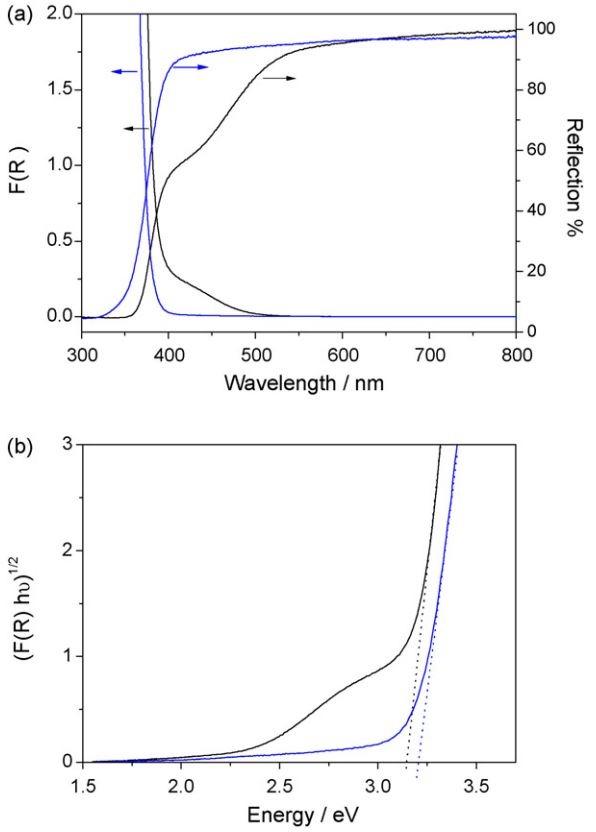

Fig. 3. a) Diffuse reflection spectra and absorption spectra converted by the Kubelka-Munk function of the TPS powder (black lines) and pristine TiO_2 (blue lines) powder, respectively. b) Tauc polts of the TPS powder (black line) and pristine TiO_2 powder (blue line), respectively, for estimation of band gap values. (For interpretation of the references to color in this figure legend, the reader is referred to the web version of the article.)

3.3. Photoelectrochemical studies

The photoelectrochemical method was employed to study the oxidation ability of VL-irradiated TPS film electrodes. Before measurement, the film electrodes were exposed to intense UV light (30 mW cm^{-2}) for over 30 min to remove any organic contamination on electrode surface. Current density j vs voltage V of the TPS electrode was at first measured in 0.1 M $NaClO_4$ (pH ~ 5) in the dark and under irradiation, respectively. As shown in Fig. 5, the dark current is negligible in a range from −0.3 V to +0.9 V; below −0.3 V, the reduction of water is observed. An anodic photocurrent at a potential over −0.43 V was observed when the electrode was irradiated with Xe lamp, corresponding to the photo-oxidation of water. The anodic photocurrent was also observed when the electrode was irradiated with the visible light ($\lambda > 450$ nm). However, it was tens of time smaller than that observed under full Xe irradiation. Note that no oxygen bubble could be observed during the scan since the photocurrent is too small and the film electrode itself is porous. But here we ascribe the generation of anodic current under visible irradiation to the photo-oxidation of water, for any organic contaminants should be removed in the pre-irradiation of film electrode with intense UV light. When the TPS electrode was irradiated with $\lambda > 500$ nm visible light, no appreciable anodic photocurrent could be observed, though the electrode showed absorption in the range over 500 nm. The above-mentioned experiments were repeated for several times and the results were reproducible.

Phenol (100 mg L^{-1}) appeared to increase the anodic photocurrent of the electrode under both Xe lamp and VL irradiation, indicating the substances was oxidized on irradiated electrode surface. As shown in Fig. 6a, addition of phenol improved the photocurrent response by a factor of ~3 under Xe lamp irradiation. The increasing factors under $\lambda > 450$ nm VL irradiation were ~2, smaller than that under Xe lamp irradiation. Since Xe lamp emits both UV light and visible light, the results indicate that the

Table 2
Initial rate constants of phenol degradation in the TPS suspensions (2 g L^{-1} and 20 g L^{-1}) under simulated solar irradiation and visible irradiation ($\lambda > 400$ nm).

	Rate constant/min^{-1}	
	2 g L^{-1} TPS	20 g L^{-1} TPS
Solar light	2.8×10^{-3}	6.8×10^{-3}
$\lambda > 400$ nm	1.2×10^{-3}	4.2×10^{-3}

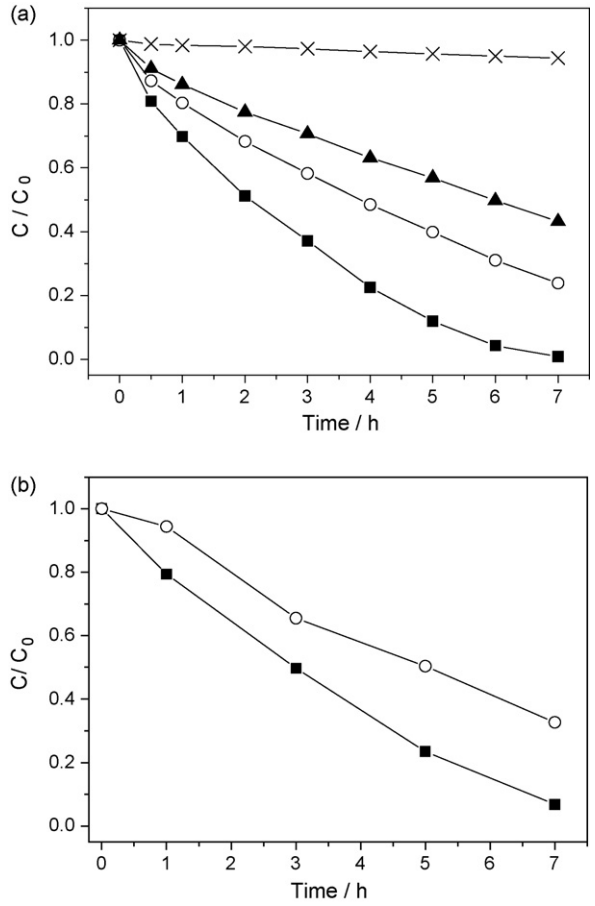

Fig. 4. a) Degradation of phenol in the TPS suspension (20 g L^{-1}) under simulated solar irradiation (Square) and visible irradiations (Circle: λ > 400 nm; Triangle: λ > 450 nm; X mark: λ > 565 nm). b) Mineralization of phenol in the TPS suspension under simulated solar irradiation (Square) and visible irradiations (λ > 400 nm, Circle).

photoelectrochemical oxidation of phenol is more efficient on a UV-excited TPS electrode than a VL-excited electrode.

Maleic acid, an open-ring oxidized product of phenol [47], also appeared to increase the anodic photocurrent response of the TPS electrode under both Xe and visible irradiation (Fig. 6b), indicating the substance was also able to be oxidized on irradiated

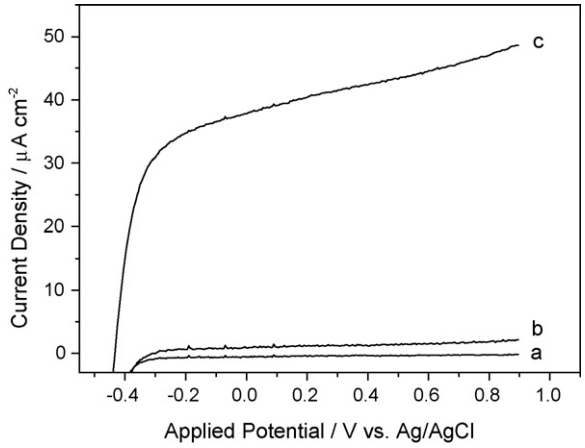

Fig. 5. *j–V* curves of the TPS electrode measured in 0.1 M $NaClO_4$ (pH ~ 5) in the dark (a), under λ > 450 nm irradiation (b) and full illumination of Xe lamp (c). The scanning was from +0.9 V to −0.5 V vs Ag/AgCl at a rate of 50 mV s^{-1}.

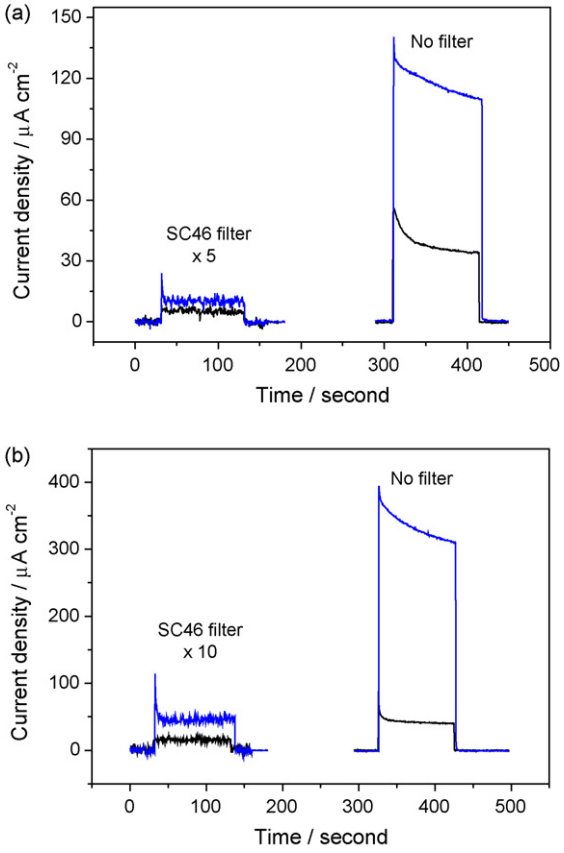

Fig. 6. Anodic photocurrent responses of the TPS electrode under filtered irradiation (SC46 filter, λ > 450 nm) and full irradiation of Xe lamp. The black lines and blue lines were recorded a) in the absence and presence of phenol pollutant (100 mg L^{-1}) and b) in the absence and presence of maleic acid pollutant (100 mg L^{-1}). (For interpretation of the references to color in this figure legend, the reader is referred to the web version of the article.)

TPS electrode. The phenomena are consistent with the observed photocatalytic mineralization of phenol under both solar and VL irradiation. Addition of maleic acid (100 mg L^{-1}) to 0.1 M $NaClO_4$ electrolyte solution increased the photocurrent response by a factor of ~8 under Xe lamp irradiation, which is larger than the ~3 of phenol. The more efficient oxidation of maleic acid than phenol can be explained by the difference in oxidation pathways: phenol is oxidized by an indirect way, i.e. by deeply trapped holes, surface-bound oxygen-centered radicals, since it is only weakly adsorbed on TiO_2 surface; maleic acid, however, can be oxidized by free or shallowly trapped holes besides deeply trapped holes and surface-bound oxygen-centered radicals, since it is strongly adsorbed on TiO_2 surface.

Under λ > 450 nm VL irradiation, maleic acid increased the photocurrent response by factors of ~3. The value is smaller than that under Xe lamp irradiation, same as the results of photoelectrochemical oxidation of phenol.

In a photoelectrochemical process on the TPS film electrode, photogenerated holes or related oxidized species participate in the oxidation of water or organic substances, while the photogenerated electrons are extracted to the external circuit as an observed photocurrent. In the backside irradiation mode, the collection efficiency of UV-generated electrons should be greater than the VL-generated electrons for the TPS electrode, since the former has a shorter diffusion length than the latter due to the different absorption coefficients in UV and visible light regions. As a result, VL (λ > 450 nm)-stimulated photocurrent of a TPS electrode was tens of time smaller than the photocurrent generated under full

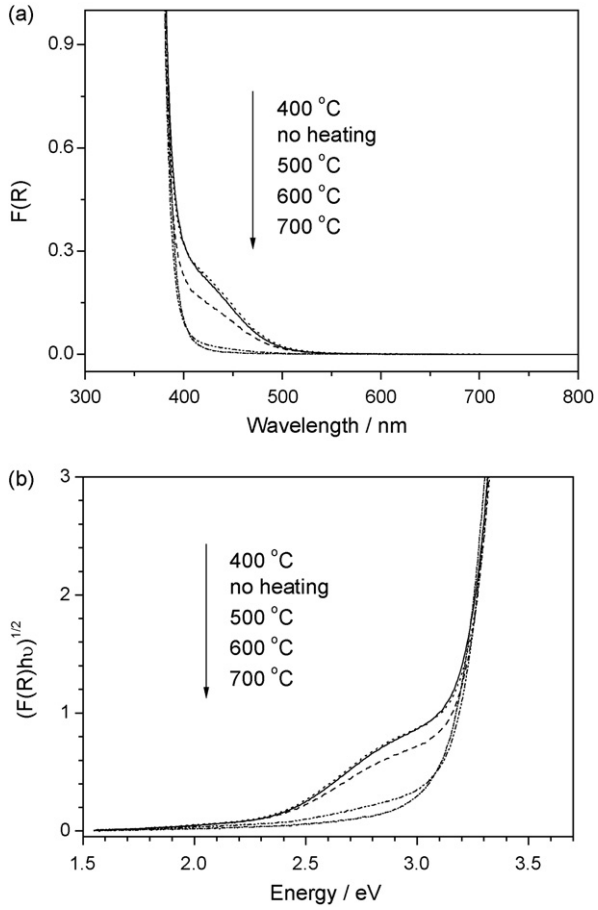

Fig. 7. a) The absorption spectra of TPS powders calcined at 400, 500, 600, and 700 °C, respectively converted from the diffuse reflection spectra by the Kubelka-Munk function. The spectrum of the non-calcined TPS powder is also shown in the figure for comparison. b) Tauc plots of the same powders in a) for estimation of band gap values.

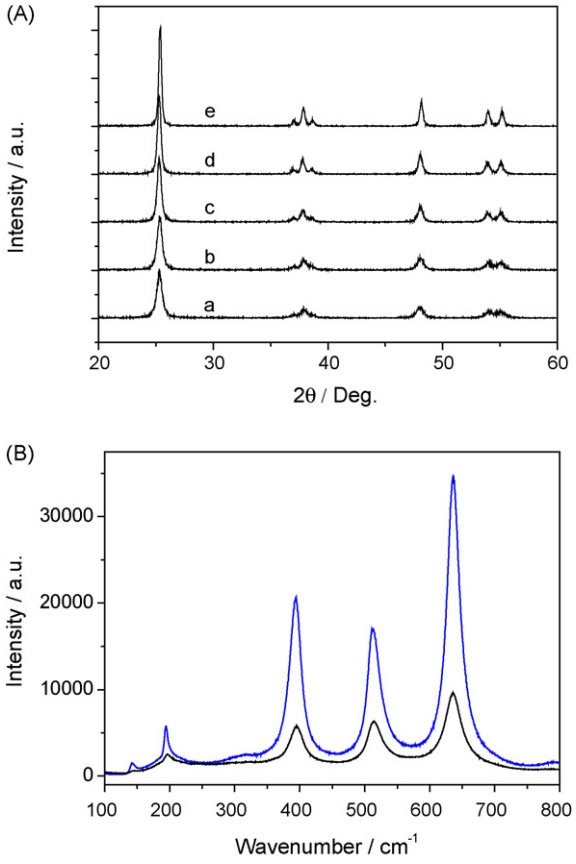

Fig. 8. A) XRD patterns of a) TPS, b) TPS 400, c) TPS 500, d) TPS 600, e) TPS 700 powders. B) Raman spectra of the TPS powder (black line) and the powder calcined at 700 °C (blue line). (For interpretation of the references to color in this figure legend, the reader is referred to the web version of the article.)

irradiation of Xe lamp. For comparison, VL ($\lambda > 450$ nm)-stimulated degradation of phenol contributed about one-third of the total solar degradation in a TPS suspension (2 g L^{-1}).

The TPS electrode did not generate appreciable anodic photocurrent under $\lambda > 500$ nm irradiation in the presence of phenol and maleic acid, suggesting the photoactivity of the TPS material, if any, was negligible in that wavelength region. The weak absorption of the TPS material over 500 nm may generate highly localized charge carriers so that they are silent in generation of photocurrent.

3.4. Calcination effect

We calcined the TPS powder in air at several temperatures and measured the diffuse reflection spectra of the calcined powders. As shown in Fig. 7, the absorption in the visible light region change negligibly for the powder calcined at/below 400 °C. The TPS powder calcined at higher temperature, however, exhibited decreased absorption in the visible light region. The TPS powder turned to white color after calcination at 700 °C, and the sample lost the N_{1s} band around 400 eV in the XPS spectrum. These results suggest that the TPS powder is not stable against heat treatment over 400 °C and will lose nitrogen dopants during calcinations at high temperature. Similar results of thermal instability were also reported by Anpo et al. on a N-doped TiO_2 film prepared by magnetron sputtering [20].

The TPS powder remained anatase morphology after calcination up to 700 °C, as shown in Fig. 8. But calcinations did cause the growth of TPS particles and the decrease of BET surface area, as shown in Table 3. The calcined samples showed stronger phonon peaks in Raman spectra with narrower line width, which indicated increased crystallinity after calcinations [44]. Notable growth of particles was observed for calcinations over 500 °C, but the BET surface area was decreased even for a calcination temperature of 400 °C probably due to the necking of TPS particles (Table 3).

We studied the photocatalytic activities of calcined TPS powders for phenol degradation and compared them with that of the non-calcined powder. As shown in Fig. 9, calcinations over 500 °C led to the decrease of activity in the VL irradiation ($\lambda > 400$ nm), but improved the activity in simulated solar irradiation. Calcination at 400 °C did not cause appreciable change in activity, and thus the data were not shown in the figure. The sample calcined at 600 °C showed the best activity in solar irradiation, despite its weak activity in VL irradiation. The results demonstrated that partial removal of the nitrogen dopants may improve the photocatalytic activity of the TPS powder under UV irradiation, suggesting that these dopants act as recombination centers for the UV-generated electron and hole carriers.

Table 3
Grain size and BET surface area of TPS powders after calcinations at various temperatures.

Calcination temperature/°C	Grain size/nm	BET surface area/m^2 g^{-1}
–	16.4	97.4
400	17.4	63.6
500	19.7	58.0
600	24.4	30.2
700	30.2	11.1

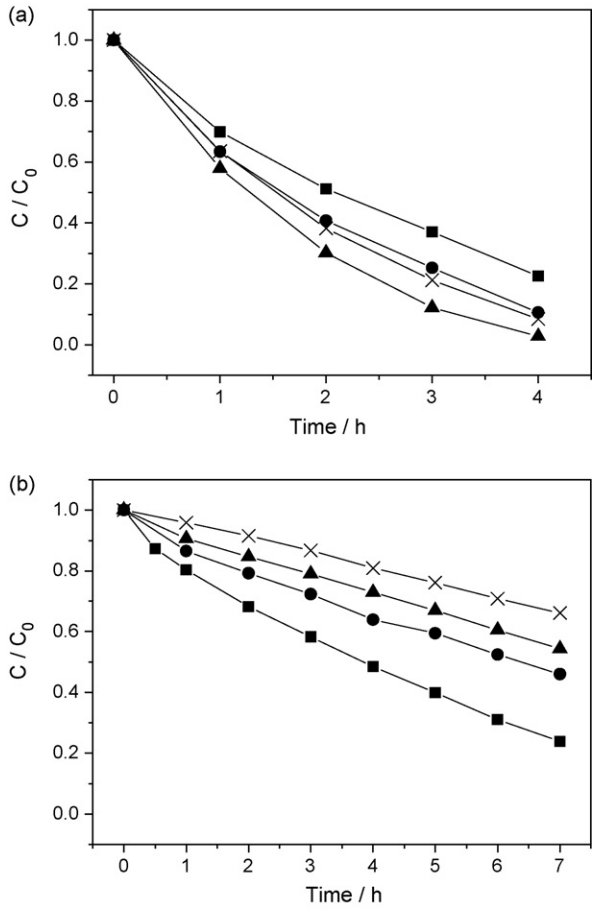

Fig. 9. Degradation of phenol in the suspension of TPS (Square), TPS 500 (Diamond), TPS 600 (Triangle), TPS 700 (X mark) under a) simulated solar irradiation and b) $\lambda > 400$ nm visible irradiation. The suspension concentration is 20 g L^{-1}.

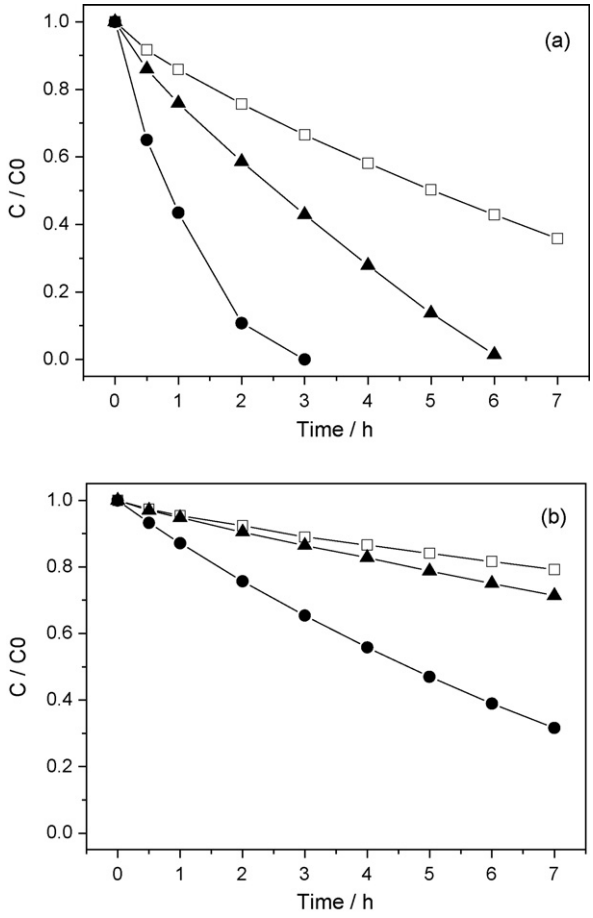

Fig. 10. Degradation of phenol in the TPS (Square) and Pt-TPS (Circle: 0.2 wt% Pt; Triangle: 1 wt% Pt) suspension (2 g L^{-1}) under a) simulated solar irradiation and b) visible irradiation ($\lambda > 450$ nm).

3.5. Effect of Pt deposition

Pt is frequently used to improve the activity of pristine TiO_2 photocatalyst, since it can improve the charge separation after UV excitation [38–40]. Therefore, it is interesting for us to investigate the effect of Pt on the photocatalytic activity of TPS under either VL or solar irradiation. We deposited Pt nanoparticles on TPS powder by photocatalytic reduction, and studied the photocatalytic activities of Pt-deposited TPS (Pt-TPS) powder under solar irradiation and VL irradiation, respectively. The Pt nanoparticles were 4–5 nm as observed by TEM. Pt-TPS powders exhibited improved activity for phenol degradation under simulated solar light compared to the TPS powder, as shown in Fig. 10 and Table 4. A 0.2 wt% of Pt intriguingly improved the degradation rate by a factor of 5.0, while a 1 wt% of Pt improved the degradation rate by a factor of 1.7. Pt nanoparticles were believed to improve the charge separation of TiO_2 photocatalysts, which is primarily important for photocatalytic reactions. Photogenerated electrons can be captured efficiently by Pt nanoparticles and there they are transferred to dioxygen to produce superoxide, hydrogen peroxide or water. But excessive deposition of Pt particles may block active sites on the TiO_2 surface and thus do harm to the photodegradation rate [39]. Therefore, a 0.2 wt% of Pt performed better than a 1 wt% of Pt for the TPS powder. Pt-TPS powders also improved the degradation of phenol under VL irradiation ($\lambda > 450$ nm), but the improvement was less than that under simulated solar light. A 0.2 wt% of Pt improved the phenol degradation by a factor of 2.6, while that was 1.1 for 1 wt% of Pt. The higher different improving factors of Pt under solar than VL irradiation is interesting, and has not been mentioned before to the best of our knowledge. This suggests different charge separation and diffusion mechanisms are involved in VL and solar (UV) excitation of the TPS material, consistent with the photoelectrochemical and photocatalytic studies above-mentioned.

Table 4
Initial rate constants of phenol degradation in the TPS and Pt-TPS suspensions (2 g L^{-1}) under simulated solar irradiation and visible irradiation ($\lambda > 450$ nm).

	Rate constant/min^{-1}		
	No Pt	0.2 wt% Pt	1 wt% Pt
Solar light	2.8×10^{-3}	1.4×10^{-2}	4.8×10^{-3}
$\lambda > 450$ nm	8.8×10^{-4}	2.3×10^{-3}	9.8×10^{-4}

In control experiments, we deposited Pt on pristine TiO_2 photocatalyst (ST-01) and studied the photocatalytic activity of the Pt-TiO_2 photocatalysts by phenol degradation. We found that a 0.2 wt% of Pt only improved the activity of ST-01 by a factor of 1.9 (Fig. 11), a normal value in comparison with previous reports on degradation of organic pollutants with Pt-deposited TiO_2 photocatalysts [38–40]. The enhancing factor, however, is much lower than that observed on the Pt (0.2 wt%)-TPS. As a result, the Pt-TPS photocatalyst exhibited better activity for solar degradation of phenol in Fig. 11 than the pristine TiO_2 (ST-01) photocatalyst with or without Pt deposition, despite the poorer activity of the TPS photocatalyst itself. Our results thus suggest that N-doped TiO_2 photocatalysts are promising materials for solar or

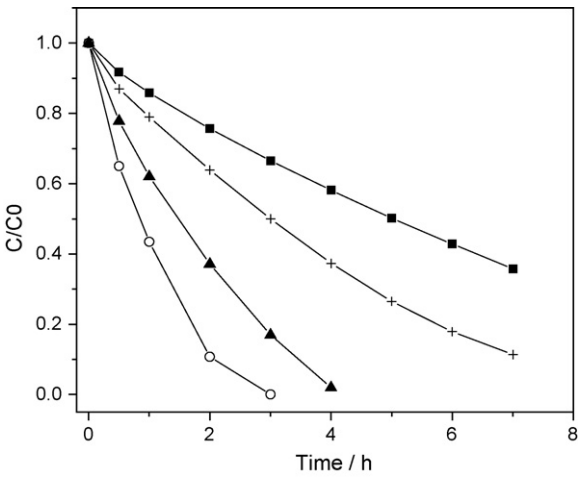

Fig. 11. Comparison on the degradation rates of phenol in the TPS (Square), ST-01 (X mark), 0.2 wt% Pt-TPS (Circle), and 0.2 wt% Pt-ST-01 (Triangle) suspension (2 g L^{-1}) under simulated solar irradiation.

VL degradation of organic pollutants, provided the recombination of photogenerated carriers could be efficiently suppressed.

Recent experimental and theoretical studies have given solid evidences that nitrogen dopants in a doping level of several percentage introduce discrete mid-gap states above the valence band (VB) edge of TiO_2 [16–19,33–36]. As excited by VL photons, electrons are promoted to the conduction band (CB), while holes are left in the mid-gap states. Because of the discrete nature of these mid-gap states, the mobility of VL-generated holes is far lower than that of UV-generated holes in VB. As a result, the VL-generated hole tends to recombine with CB electron than do interfacial oxidation reaction. This issue has been pointed out in the transient spectroscopic studies on N-doped TiO_2 powder by Tachikawa et al. [48]. Moreover, the mid-gap states can work as efficient traps for the UV-generated VB holes, which increased their recombination probability with CB electrons. In the sum, the N-doped TiO_2 material suffers more serious charge recombination than pristine TiO_2 material under excitation. Therefore, the TPS showed poorer photocatalytic activity than pristine TiO_2 (ST-01) under solar irradiation, despite that the former can absorb and utilize visible light. However, when the charge recombination in the TPS was suppressed by a small amount of Pt nanoparticles, the activity of the TPS was improved so much that it even exceeded that of the Pt-deposited pristine TiO_2.

It is still unclear why Pt improved the activity of the TPS more under solar irradiation than under VL irradiation ($\lambda > 450$ nm). Very recently, Morikawa et al. reported Cu and Pt could improve the photocatalytic mineralization rate of gaseous acetaldehyde with $TiO_{2-x}N_x$ under VL irradiation, but no results related to solar irradiation were reported there [49,50]. They assume a synergic photocatalytic and thermocatalytic decomposition and gaseous acetaldehyde on the surface of Pt-deposited $TiO_{2-x}N_x$ [49,50]. Their assumption, however, is not applicable to our studies, since we observed Pt cocatalyst influenced the photocatalytic degradation of phenol under solar and VL irradiation in different way. One possible explanation for our experimental observations thereby concerns the different mobility of holes in VB and in mid-gap states. The VB holes move quickly and are able to move from the interior to the surface of a TiO_2 nanoparticle in a scale of picosecond [51]. Holes in the mid-gap states, however, move slowly through the communication with other mid-gap states or VB states [17], and thus the mobility of holes in mid-gap states is strongly influenced by the depth of these states in the band gap. In a conventional UV-stimulated photocatalytic event concerning VB holes, the rate-determining step is the reduction of molecular oxygen with photogenerated CB electrons, which takes over tens to hundreds of microseconds [52–54]. However, in the case of VL-excited N-doped TiO_2, the migration of holes in mid-gap states is so slow that it may take a long time from the interior to the surface of particles that is comparable or even longer than that takes for transferring CB electrons to oxygen. As a result, Pt nanoparticles may have different impact on the charge recombination behavior of VB and mid-gap holes.

In a previous study, Emeline et al. reported quantum yields of 8% and 12% for phenol degradation on the TPS powder irradiated with 436 nm and 365 nm monochromatic light, respectively [55]. These values were quite comparable to that on Degussa P_{25} powder (14% at 365 nm). However, Emeline's measurements were conducted in the light-limit conditions, i.e. very low light intensity and high phenol concentration, which has great advantages over the light-rich conditions of actual photocatalytic systems in minimizing charge recombination. Therefore, these values represent the maximum quantum yields a phenol degradation process can reach on irradiated photocatalysts, which imply that the TPS would perform better than pristine TiO_2 photocatalysts in solar photocatalysis provided the charge recombination was suppressed sufficiently. Therefore, future applications of the TPS photocatalyst, or other VL responsive TiO_2 photocatalysts should consider how to improve the charge separation of photogenerated carriers. One promising way is to couple those photocatalysts with noble metal, such as Pt, like the present study or other semiconducting materials such as SnO_2 and TiO_2 (rutile). Actually, we have shown that a 0.2 wt% Pt intriguingly improves the solar degradation of phenol by a factor of 5, and we believe that even greater improvement can be obtained with optimizing the conditions of Pt deposition.

4. Conclusion

A commercial N-doped TiO_2 (TPS) powder was studied as a model material by photocatalytic and photoelectrochemical methods in order to evaluate the photoactivity of N-doped TiO_2 materials and the possibility of their applications in solar and VL photocatalysis. Our studies clearly show that nitrogen doping which causes the generation of mid-gap states offers the VL photocatalytic activity to TiO_2. The TPS is able to utilize visible light with a wavelength shorter than 500 nm to oxidize and mineralize phenol. However, the VL activity of the TPS is lower than that under UV irradiation, due to the discrete nature of mid-gap states. Our studies also show that the nitrogen mid-gap states have a negative effect to the photocatalytic process based on UV-stimulated VB holes due to the enhancement on charge recombination. A small amount of Pt (0.2 wt%) deposited on the TPS powder, however, was able to greatly improve the photocatalytic activity under both solar and VL irradiation, and makes the material promising for solar photocatalysis. Our studies also show that calcining the TPS at/over 500 °C oxidizes the material and reduces the VL photocatalytic activity. Though the present study is carried out on a commercial N-doped TiO_2 material, yet the conclusion of this study should be general for N-doped TiO_2, or other kinds of nonmetal-doped TiO_2 materials.

Acknowledgements

This work was supported by the Asia S&T Strategic Cooperation Program and a Grant-in-Aid for Scientific Research on Priority Areas (417) from the Ministry of Education, Culture, Sports, Science and Technology (MEXT) of the Japanese Government, and by the Core Research for Evolutional Science and Technology (CREST) Program of the Japan Science and Technology (JST) Agency.

References

[1] A. Fujishima, K. Honda, Nature 238 (1972) 37.
[2] A. Fujishima, K. Kohayakawa, K. Honda, J. Electrochem. Soc. 122 (1975) 1487.
[3] B. O'Regan, M. Grätzel, Nature 335 (1991) 737.
[4] A. Hagfeldt, M. Grätzel, Chem. Rev. 95 (1995) 49.
[5] M. Grätzel, J. Photochem. Photobiol. C: Photochem. Rev. 4 (2003) 145.
[6] A. Fujishima, X.-T. Zhang, Proc. Jpn. Acad. Ser. B 81 (2005) 33.
[7] M.R. Hoffmann, S.T. Martin, W. Choi, D.W. Bahnemann, Chem. Rev. 95 (1995) 69.
[8] A. Heller, Acc. Chem. Res. 28 (1995) 503.
[9] U. Stafford, K.A. Gray, P.V. Kamat, Chem. Rev. 3 (1996) 77.
[10] A. Fujishima, K. Hashimoto, T. Watanabe, TiO_2 Photocatalysis Fundamentals and Applications, BKC Inc., 1999.
[11] A. Fujishima, T.N. Rao, D.A. Tryk, J. Photochem. Photobiol. C: Photochem. Rev. 1 (2000) 1.
[12] A. Fujishima, X. Zhang, C. R. Chimie 9 (2006) 750.
[13] K. Hashimoto, H. Irie, A. Fujishima, Jpn. J. Appl. Phys. 44 (2005) 8269.
[14] R. Asahi, T. Morikawa, T. Ohwaki, K. Aoki, Y. Taga, Science 293 (2001) 269.
[15] S. Sakthivel, H. Kisch, ChemPhysChem 4 (2003) 487.
[16] H. Irie, Y. Watanabe, K. Hashimoto, J. Phys. Chem. B 107 (2003) 5483.
[17] G.R. Torres, T. Lindgren, J. Lu, C.-G. Granqvist, S.-E. Lindquist, J. Phys. Chem. B 108 (2004) 5995.
[18] R. Nakamura, T. Tanaka, Y. Nakato, J. Phys. Chem. B 108 (2004) 10617.
[19] M. Mrowetz, W. Balcerski, A.J. Colussi, M.R. Hoffmann, J. Phys. Chem. B 108 (2004) 17269.
[20] M. Kitano, K. Funatsu, M. Matsuoka, M. Ueshima, M. Anpo, J. Phys. Chem. B 110 (2006) 25266.
[21] E.A. Reyes-Garcia, Y. Sun, K. Reyes-Gil, D. Raftery, J. Phys. Chem. C 111 (2007) 2738.
[22] Y. Nakano, T. Mnorikawa, T. Ohwaki, Y. Taga, Appl. Phys. Lett. 86 (2005) 132104.
[23] H. Irie, Y. Watanabe, K. Hashimoto, Chem. Lett. 32 (2003) 772.
[24] B. Neumann, P. Bogdanoff, H. Tributsch, S. Sakthivel, H. Kisch, J. Phys. Chem. B 109 (2005) 16579.
[25] J.H. Park, S. Kim, A.J. Bard, Nano Lett. 6 (2006) 24.
[26] S.-W. Hsu, T.-S. Yang, T.-K. Chen, M.-S. Wong, Thin Solid Films 515 (2007) 3521.
[27] T. Umebayashi, T. Yamaki, S. Tanaka, K. Asai, Chem. Lett. 32 (2003) 330.
[28] T. Umebayashi, T. Yamaki, H. Itoh, K. Asai, Appl. Phys. Lett. 81 (2002) 454.
[29] T. Ohno, T. Mitsui, M. Matsumura, Chem. Lett. 32 (2003) 364.
[30] W. Zhao, W. Ma, C. Chen, J. Zhao, Z. Shuai, J. Am. Chem. Soc. 126 (2004) 4782.
[31] J.C. Yu, J.G. Yu, W.K. Ho, Z.T. Jiang, L.Z. Zhang, Chem. Mater. 14 (2002) 3808.
[32] D. Li, H. Haneda, S. Hishita, N. Ohashi, Chem. Mater. 17 (2005) 2596.
[33] M. Batzill, E.H. Morales, U. Diebold, Phys. Rev. Lett. 96 (2006) 026103.
[34] A. Nambu, J. Graciani, J.A. Rodriguez, Q. Wu, E. Fujita, J. Chem. Phys. 125 (2006) 094706.
[35] C. Di Valentin, G. Pacchioni, A. Selloni, S. Livraghi, E. Giamello, J. Phys. Chem. B 109 (2005) 11414.
[36] S. Livraghi, M.C. Paganini, E. Giamello, A. Selloni, C. Di Valentin, G. Pacchioni, J. Am. Chem. Soc. 128 (2006) 15666.
[37] H.M. Yates, M.G. Nolan, D.W. Sheel, M.E. Pemble, J. Photochem. Photobiol. A: Chem. 179 (2006) 213.
[38] B. Sun, A.V. Vorontsov, P.G. Smirniotis, Langmuir 19 (2003) 3151.
[39] S. Sakthivel, M.V. Shankar, M. Palanichamy, B. Arabindoo, D.W. Bahnemann, V. Murugesan, Water Res. 38 (2004) 3001.
[40] D. Hufschmidt, D. Bahnemann, J.J. Testa, C.A. Emilio, M.I. Litter, J. Photochem. Photobiol. A: Chem. 148 (2002) 223.
[41] K. Chiang, T.M. Lim, L. Tsen, C.C. Lee, Appl. Catal. B 261 (2004) 225.
[42] N.C. Saha, H.G. Tompkins, J. Appl. Phys. 72 (1992) 3072.
[43] T. Ohsaka, F. Izumi, Y. Fujiki, J. Raman Spectrosc. 7 (1978) 321.
[44] W.F. Zhang, Y.L. He, M.S. Zhang, Z. Yin, Q. Chen, J. Phys. D: Appl. Phys. 33 (2000) 912.
[45] Z. Lin, A. Orlov, R.M. Lambert, M.C. Payne, J. Phys. Chem. B 109 (2005) 20948.
[46] J.M. Herrmann, Top. Catal. 34 (2005) 49.
[47] A. Eftaxias, J. Font, A. Fortuny, J. Giralt, A. Fabregat, F. Stüber, Appl. Catal. B: Environ. 33 (2001) 175.
[48] T. Tachikawa, Y. Takai, S. Tojo, M. Fujitsuka, H. Irie, K. Hashimoto, T. Majima, J. Phys. Chem. B 110 (2006) 13158.
[49] T. Morikawa, Y. Irokawa, T. Ohwaki, Appl. Catal. A: General 314 (2006) 123.
[50] T. Morikawa, T. Ohwaki, K. Suzuki, S. Moribe, S. Tero-Kubota, Appl. Catal. B: Environ. 83 (2008) 56.
[51] Y. Tamaki, A. Furube, M. Murai, K. Hara, R. Katoh, M. Tachiya, J. Am. Chem. Soc. 128 (2006) 416.
[52] T. Yoshihara, R. Katoh, A. Furube, Y. Tamaki, M. Murai, K. Hara, S. Murata, H. Arakawa, M. Tachiya, J. Phys. Chem. B 108 (2004) 3817.
[53] A.M. Peiro, C. Colombo, G. Doyle, J. Nelson, A. Mills, J.R. Durrant, J. Phys. Chem. B 110 (2006) 23255.
[54] A. Yamakata, T. Ishibashi, H. Onishi, J. Phys. Chem. B 105 (2001) 7258.
[55] A.V. Emeline, X. Zhang, M. Jin, T. Murakami, A. Fujishima, J. Phys. Chem. B 110 (2006) 7409.